Ion Transport in an Immortalized Rat Submandibular Cell Line SMG-C6 (44550)

ROBERT CASTRO,*·[1] LORNELL BARLOW-WALDEN,* TRUDI WOODSON,* JAY D. KERECMAN,† GUO H. ZHANG,* AND J. RICARDO MARTINEZ‡

*Department of Pediatrics, University of Texas Health Science Center at San Antonio, San Antonio, Texas 78284–7812; †Department of Pediatrics, Wilford Hall Medical Center, San Antonio, Texas 78236–5000; and ‡National Institute of Dental and Craniofacial Research, National Institutes of Health, Bethesda, Maryland 20892–2190

Abstract. **The immortalized rat submandibular epithelial cell line, SMG-C6, cultured on porous tissue culture supports, forms polarized, tight-junction epithelia facilitating bioelectric characterization in Ussing chambers. The SMG-C6 epithelia generated transepithelial resistances of 956±84Ω.cm^2 and potential differences (PD) of −16.9 ± 1.5mV (apical surface negative) with a basal short-circuit current (I_{sc}) of 23.9 ± 1.7 μA/cm^2 (n = 69). P2 nucleotide receptor agonists, ATP or UTP, applied apically or basolaterally induced a transient increase in I_{sc}, followed by a sustained decreased below baseline value. The peak ΔI_{sc} increase was partly sensitive to Cl$^-$ and K$^+$ channel inhibitors, DPC, glibenclamide, and tetraethylammonium (TEA) and was completely abolished following Ca^{2+} chelation with BAPTA or bilateral substitution of gluconate for Cl$^-$. The major component of basal I_{sc} was sensitive to apical Na$^+$ replacement or amiloride (half-maximal inhibitory concentration 392 n*M*). Following pretreatment with amiloride, ATP induced a significantly greater I_{sc}; however, the poststimulatory decline was abolished, suggesting an ATP-induced inhibition of amiloride-sensitive Na$^+$ transport. Consistent with the ion transport properties found in Ussing chambers, SMG-C6 cells express the rat epithelial Na$^+$ channel α-subunit (α-rENaC). Thus, cultured SMG-C6 cells produce tight polarized epithelia on permeable support with stimulated Cl$^-$ secretory conductance and an inward I_{sc} accounted for by amiloride-sensitive Na$^+$ absorption.** [P.S.E.B.M. 2000, Vol 225:39–48]

Studies using intact salivary glands or freshly isolated cells have contributed to our understanding of salivary secretion and modification; however, elucidating the specific site(s) of ion transport regulation is difficult from heterogeneous cellular preparations. Isolated cultures of homogeneous salivary epithelial cells would allow for more precise measurements of regulatory ion transport under controlled conditions. Normal (nontumor-derived) epithelial cells from the salivary glands have been isolated and maintained in culture (1–3). Yet, even under optimal conditions, functional studies from primary salivary cultures are restricted due to limited life span or terminal differentiation (4). Continuous cell lines derived from rodent salivary glands have been established, demonstrating stable morphology and function (5), including tight junctions and polarized membrane proteins consistent with vectorial ion transport (6, 7). More recently Quissell *et al.* have reported the establishment of SV40-transformed rat parotid (8) and submandibular (9) gland cell lines of acinar origin. The parotid cells (Par-C10) grown on porous tissue culture supports formed tight, polarized epithelial monolayers, permitting characterization of neurotransmitter-regulated anion secretion (10).

The SMG-C6 cell line derived from rat submandibular acinar glands expresses specific acinar cell proteins and retains receptor-stimulated mobilization of intracellular signaling elements (Ca^{2+} and cAMP) with varying consistency compared with intact salivary glands or freshly isolated cells (9). Therefore, the current study was performed to characterize basal and stimulated ion transport processes from this immortalized homogeneous preparation and to

This work was supported by the Department of Pediatrics and Medical Hispanic Center of Excellence, University of Texas Health Science Center, San Antonio, Texas.

[1] To whom requests for reprints should be addressed at the Department of Pediatrics, University of Texas Health Science Center, 7703 Floyd Curl Drive, San Antonio, TX 78284–7812. E-mail: castror@uthscsa.edu

Received December 2, 1999. [P.S.E.B.M. 2000, Vol 225]
Accepted April 24, 2000.

0037-9727/00/2251-0039$15.00/0

compare them with properties found in acinar epithelium. SMG-C6 cells cultured on collagen-coated polycarbonate filters displayed clear evidence of polarization with stable transepithelial resistance, facilitating their bioelectric characterization in Ussing chambers. Under short-circuit conditions, the cell line exhibited agonist-stimulated Cl^- secretory conductance. However, not commonly associated with acinar transport function, amiloride-sensitive apical Na^+ absorption in conjunction with the expression of rat epithelial Na^+ channels (rENaC) was demonstrated.

Materials and Methods

Materials. DMEM/F12, fetal bovine serum (FBS) and trace element mix were obtained from Gibco (Grand Island, NY). Transferrin and epidermal growth factor (EGF) were obtained from JRH Biosciences (Lenexa, KS). Insulin was obtained from Novo Nordisk Pharmaceuticals (Princeton, NJ). Polycarbonate Snapwell filters were obtained from Costar (Cambridge, MA). The drugs used were: amiloride, dimethylamiloride, benzamil, acetylcholine, ouabain, ATP, UTP, dibutyryl-cAMP (Bt_2-cAMP), tetraethylammonium (TEA), bumetanide, isoproterenol, glibenclamide (Sigma Chemical Co, St. Louis, MO), diphenylamine-2-carboxylic acid (DPC; Fluka Chemical Corp, Ronkonkoma, NY), 1,2-bis-(2-aminophenoxy)ethane N,N,N′,N′-tetraacetic acid (BAPTA-AM; Molecular Probes, Eugene, OR), and 5-(N-ethyl-N-isopropyl)-amiloride (EIPA; Research Biochemical, Natick, MA).

Cell Culture. SMG-C6 cells (passages 22–34) were seeded at a density of 2.5×10^5 cells/cm^2 on Snapwell tissue culture–treated filters (diameter 12mm, pore size 0.4 μm) coated with 1.0 μg/cm^2 of human collagen type-I (Becton Dickinson, Franklin Lakes, NJ). The modified culture medium (8, 9) used was DMEM/F12 (1:1 mixture) with 2.5% FBS supplemented with trace element mix, 5 μg/ml transferrin, 1.1 μ*M* hydrocortisone, 0.1 μ*M* retinoic acid, 2.0 n*M* T_3, 5 μg/ml insulin, 80 ng/ml EGF, 100 U/ml penicillin, and 100 μg/ml streptomycin.

Transepithelial Transport Studies. Transepithelial resistances (R_t) of the SMG-CG monolayers grown on permeable filters were serially measured by an EVOM-G (World Precision Instrument, WPI, Sarasota, FL). Filters exhibiting an $R_t > 400\ \Omega.cm^2$ were placed in a modified Ussing chamber (Costar, Cambridge, MA) equipped with Ag/AgCl electrodes and bathed with Krebs-Ringer bicarbonate (KRB) medium containing (in m*M*): 120 NaCl, 2.5 K_2HPO_4, 0.6 KH_2PO_4, 1.2 $CaCl_2$, 1.2 $MgCl_2$, 20 $NaHCO_3$, and 10 glucose at pH 7.4. For ion replacement studies, all Cl^- and Na^+ in KRB were replaced with an equivalent amount of gluconate or choline, respectively.

The media were air-lifted with 5% CO_2/21% O_2, and the temperature was maintained at 37°C. Using a DVC-1000 Voltage/Current Clamp (WPI) with automatic fluid resistance compensation, stable baseline potential difference (PD) was measured. After equilibration (10–15 min), the monolayer's PD was clamped to 0 mV, and short-circuit current (I_{sc}) was continuously recorded. Every 30 sec, the monolayer was clamped to 1 mV for 0.5 sec so that measured changes in current enabled calculation of R_t using Ohm's law ($R_t = \Delta PD/\Delta I_{sc}$). Reported I_{sc} values refer to the movement of negative charge from the basolateral to apical side of the membrane, and the apical side PD is negative referenced to the basolateral side.

After reaching steady state I_{sc} values, agents known to influence ion transport were instilled into either the apical or basolateral reservoir. Peak or treatment I_{sc} values were measured at the point of maximal change immediately or following 20 min exposure, respectively. Amiloride and DPC were dissolved in DMSO and ethanol, respectively, with the final concentration of both diluents in the Ussing chamber fluid being 1:1000. Preliminary studies established the vehicle concentration at which no changes occurred in R_t. Therefore, all changes occurring in any of the transepithelial electrical parameters are due to an agent rather than its vehicle. Neither basal bioelectric properties nor the response to specific agents varied following each cell passage.

Western Blot Analysis. The SMG-C6 monolayers grown on human collagen-coated culture dishes were treated with trypsin, washed, and pelleted at 4°C in balanced salt solution. Total protein from cell lysates were resolved on 12.5% SDS-polyacrylamide gel electrophoresis, electrophoretically transferred to Optitran BA S-83 nitrocellulose membrane (Schleicher & Schuell, Keene, NH), and incubated with primary monoclonal anticytokeratin mouse antibodies C11 (Santa Cruz Biotechnology, Santa Cruz, CA), a general epithelial (pan-cytokeratin) marker, or K4.62, specific for cytokeratin 19 (Sigma). In salivary glands, cytokeratin 19 expression is restricted to differentiated epithelial cells of ductal origin (6, 11). Horseradish peroxidase–labeled secondary antibody (Sigma) and the enhanced chemiluminescence detection system (ECL Plus, Amersham Pharmacia Biotech, Piscataway, NJ) were used to visualize proteins. Extracted proteins from rat salivary glands were blotted for comparison.

RNA Isolation and Northern Analyses. Whole rat organs (submandibular glands, lung, kidney, and liver) or SMG-C6 epithelial (7×10^6 cells) RNA was extracted using Tri Reagent (Sigma Chemical Co., St. Louis, MO) and quantitated using an Ultrospec 2000 spectrophotometer (Amersham Pharmacia Biotech, Piscataway, NJ), RNA mode at 260/280nm (ratio > 1.8). The RNA was size-fractionated by electrophoresis on a 1.2% agarose gel containing 1 × MOPS and 1.1% formaldehyde. Total RNA of 20μg/lane was transferred to a Hybond-N(+) (Amersham Pharmacia Biotech, Piscataway, NJ) nylon membrane using the Turboblotter system (Schleichler & Schuell, Keene, NH). After prehybridization, blots were hybridized with ^{32}P-labeled full length α-rat epithelial Na^+ channel (α-rENaC) probe, washed with 0.2 × SSC + 0.01% SDS at 42°C for 30 min (12), and then subjected to autoradiography at −85°C for 3.5 hr (Lightening Plus intensifier screens and BioMax MS film; Eastman Kodak, Rochester, NY).

Statistical Analysis. Data were expressed as mean ± standard error (SE). Changes in response to treatment with test agents were compared with initial values (control) by paired or unpaired *t* tests as appropriate or one-way analysis of variance followed by Student-Newman-Keul multiple comparison tests to determine statistical differences between groups. A *P*-value < 0.05 was considered significant.

Results

Baseline Bioelectric Properties. Filters seeded with SMG-C6 cells (Days 3–5) exhibiting R_t values > 400 $\Omega.cm^2$ were mounted in Ussing chambers for electrophysiologic studies. Of the filters measured, >95% fit within these criteria. Under basal conditions, the R_t across the SMG-C6 epithelial filters (n = 69) was 956 ± 84 $\Omega.cm^2$ and the PD was −16.9 ± 1.5 mV (referenced to basolateral reference electrode). Transepithelial current under short-circuit condition (I_{sc}) measured 23.9 ± 1.7 $\mu A/cm^2$.

Effect of Drugs Known to Modulate Cl^- Transport. The effects of ion transport inhibitors on basal I_{sc} are summarized in Table I. The addition of the Na^+-K^+-ATPase inhibitor, ouabain (1 m*M*), to the basolateral fluid resulted in a rapid decrease in I_{sc} (36.7 ± 1.8 to 4.3 ± 3.9 $\mu A/cm^2$, $P < 0.05$). This inhibition of I_{sc} was associated with a 10.7% increase in R_t. When ouabain was added to the apical fluid, I_{sc} and R_t were not affected. Apical DPC (100 μM) or glibenclamide (100 μM), primary inhibitors of Ca^{2+}- or cAMP-activated Cl^- current (13, 14), respectively, or basolateral bumetanide (100 μM), an inhibitor of Na^+-K^+-$2Cl^-$ co-transport, did not significantly decrease basal I_{sc} value. DIDS (100 μM), a known Cl^-/HCO_3^- exchange blocker, added to the basolateral medium also did not alter basal I_{sc}. Apical DIDS lowered the I_{sc} by 23%; however, the decrease was variable and not significant. TEA, a K^+ channel inhibitor added to the basolateral bath gradually decreased basal I_{sc} by 27% ($P < 0.05$). TEA had minimal effects when added to the apical bath.

Effect of Drugs Known to Activate Ion Transport. Addition of the β-adrenergic agonist, isoproterenol (100 μM), into the basolateral bath did not significantly alter baseline I_{sc} (peak ΔI_{sc}, 2.0 ± 0.9 $\mu A/cm^2$) (Table II). Similarly, little change was noted when dibutyryl-cAMP (100 μM), a membrane permeant analog of cAMP, was added to the basolateral bath. The basolateral addition of the cholinergic agonist, acetylcholine (ACh, 100 μM), produced a transient I_{sc} increase (peak ΔI_{sc}, 6.9 ± 1.0 $\mu A/cm^2$, $P < 0.05$) with a progressive decline in I_{sc} to 79% of basal values. Addition of the P2 nucleotide receptor agonists, ATP or UTP, into the apical medium also induced a biphasic I_{sc} response with an immediate transient increase (10.9 ± 2.4 $\mu A/cm^2$ or 9.7 ± 2.4 $\mu A/cm^2$, respectively) followed by a sustained suppression to ≈ 45%–55% below the basal values (Fig. 1). Peak change in I_{sc} values in response to apical ATP or UTP concentrations from 1.0 μM to 100 μM were similar and occurred within 36.7 ± 6.0 sec (Fig. 2). The poststimulatory suppression by both P2 agonists equilibrated at 20.8 ± 1.6 min with the maximal suppression occurring at 100 μM for both agonists (Fig. 2). The changes in I_{sc} following basolateral ATP or UTP treatment did not differ from the apical biphasic response (Table II). Simultaneous treatment with ATP (apical) and isoproterenol (basolateral) produced a comparable I_{sc} peak following ATP treatment alone; however, the I_{sc} following stimulation did not significantly decline below basal values (Table II).

The effects of various ion transport blockers on the ATP-induced changes in I_{sc} are presented in Figure 3. Inhibiting the Cl^-/HCO_3^- exchanger with apical DIDS (100 μM) did not alter the ATP response; however, blocking Cl^- channels with apical DPC (100 μM) or glibenclamide (100 μM) significantly decreased the ATP-induced biphasic

Table I. Effects of Ion-Transport Inhibitors on Basal and Drug-Altered I_{sc} Values in SMG-C6 Monolayers

Drug	*n*	Basal I_{sc}	Altered I_{sc}	ΔI_{sc} (%)
Apical bath				
Ouabain (1 m*M*)	4	42.0 ± 1.5	37.7 ± 2.3	−9 ± 8
DPC (100 μM)	6	19.4 ± 4.5	17.7 ± 4.2	−7 ± 3
DIDS (100 μM)	4	33.2 ± 4.1	23.4 ± 8.0	−23 ± 5
Glibenclamide (100 μM)	4	31.8 ± 6.5	24.8 ± 5.0	−22 ± 3
Amiloride (100 μM)	6	39.8 ± 6.5	0.4 ± 0.4[a]	−101 ± 2
Amiloride (10 μM)	6	19.1 ± 4.9	0.3 ± 1.0[a]	−101 ± 5
Benzamil (100 μM)	5	28.5 ± 7.6	1.1 ± 0.5[a]	−97 ± 1
Dimethylamiloride (100 μM)	4	21.2 ± 3.9	18.3 ± 1.4	−11 ± 9
Basolateral bath				
Ouabain (100 μM)	4	36.7 ± 1.8	4.3 ± 3.9[a]	−93 ± 9
TEA (1 m*M*)	4	46.2 ± 1.9	33.3 ± 1.4[a]	−28 ± 2
Bumetanide (10 μM)	4	24.4 ± 2.2	25.4 ± 2.1	1 ± 5
DIDS (100 μM)	6	27.2 ± 1.2	27.8 ± 1.3	1 ± 2
Amiloride (100 μM)	4	16.5 ± 3.5	10.8 ± 1.8	−31 ± 11
Dimethylamiloride (100 μM)	4	16.6 ± 3.6	12.8 ± 3.3	−24 ± 6

Note. Values are mean ± SE. Final concentrations are shown in parentheses. *n*, number of experiments; I_{sc}, short-circuit current ($\mu A/cm^2$). Altered I_{sc} values were measured approximately 20 min following addition of agent. [a] $P < 0.05$ versus basal values.

Table II. Effects of Ion Transport Stimulators on Basal and Drug-Altered I_{sc} Values in SMG-C6 Monolayers

Drug	*n*	Basal I_{sc}	Altered I_{sc}	Peak ΔI_{sc}
Basolateral bath				
Isoproterenol (100 μ*M*)	6	23.3 ± 6.2	26.1 ± 1.4	2.0 ± 0.9
Dibutyryl-cAMP (100 μ*M*)	6	37.9 ± 1.9	39.0 ± 2.6	1.1 ± 0.3
Acetylcholine (100 μ*M*)	6	20.8 ± 6.3	15.3 ± 3.7	6.9 ± 1.0
ATP (100 μ*M*)	4	38.7 ± 8.6	21.8 ± 5.2	9.6 ± 1.2
UTP (100 μ*M*)	5	15.7 ± 4.7	12.2 ± 3.1	6.7 ± 1.0
Apical bath				
ATP (100 μ*M*)	9	25.3 ± 2.4	11.6 ± 2.2[a]	10.9 ± 2.4
UTP (100 μ*M*)	7	22.8 ± 3.9	10.6 ± 3.4[a]	9.7 ± 2.4
ATP (100 μ*M*) + Isoproterenol (100 μ*M*)	5	26.7 ± 2.1	25.6 ± 2.3	7.1 ± 0.8

Note. Values are mean ± SE; I_{sc}, short-circuit current (μA/cm^2); R_t transepithelial current (Ω.cm^2). Peak change in I_{sc} values (Peak ΔI_{sc}) were immediately measured following drug treatment and altered I_{sc} values were measured approximately 20 min following addition of agent.
[a] $P < 0.05$ versus baseline values.

I_{sc} responses. The Na^+-K^+-$2Cl^-$ co-transport inhibitors, bumetanide (100 μ*M*), or K^+ channel blocker, TEA (1 m*M*), added to the basolateral medium also decreased the ATP-induced peak; however, TEA did not alter the poststimulatory inhibition. Finally, incubating the SMG-C6 epithelia with the intracellular Ca^{2+} chelator, BAPTA-AM (10 μ*M*, 20 min), abolished the transient and poststimulatory I_{sc} responses to ATP (Fig. 3B).

Cl^--free medium bathing both sides of SMG-C6 monolayers significantly increased basal I_{sc} and R_t (Table III) and inhibited the ATP-induced I_{sc} increase (Fig. 4). In contrast, basolateral Cl^--free medium reduced the basal I_{sc} by 34% (28.3 ± 2.3 to 17.0 ± 3.3 μA/cm^2) and reversed the apical ATP-induced I_{sc} deflection (ΔI_{sc}, −14.0 ± 1.8 μA/cm^2), consistent with anion (Cl^-) current movement from an apical to basolateral direction.

Effect of Drugs Known to Modulate Na^+ Transport. Apical administration of amiloride at 100 m*M* completely abolished basal I_{sc} from 39.8 ± 6.4 to 0.4 ± 0.4 μA/cm^2 (Table I). At the lower concentration of 10 μ*M*, apical amiloride rapidly decreased I_{sc} from 19.1 ± 4.9 to 0.3 ± 1.0 μA/cm^2. The dose-dependent inhibitory effects of amiloride on basal I_{sc} demonstrated a half-maximal inhibitory concentration (IC_{50}) of 392 n*M* (Fig. 5A). In contrast, basal I_{sc} was unaffected by increasing concentration of EIPA, an inhibitor of amiloride-insensitive Na^+ transport (15). At an apical EIPA concentration of 100 μ*M*, I_{sc} fell to 19.5% of basal values. Apical benzamil (100 μ*M*), an amiloride analog with a high affinity for Na^+ channels, similarly depressed basal I_{sc} by 97% (Fig. 5B). Dimethylamiloride (100 μ*M*), an amiloride analog that nonspecifically blocks the Na^+-H^+ antiport (15), did not significantly lower basal I_{sc} when applied apically. Basolateral addition of 100 m*M* amiloride or dimethylamiloride (100 μ*M*) produced a smaller ≈ 30% decrease in basal I_{sc} (Table I).

The peak change in basal I_{sc} (ΔI_{sc}) caused by apical ATP was significantly greater following preincubation with apical amiloride (19.6 ± 2.8 μA/cm^2) or benzamil (34.6 ± 6.7 μA/cm^2), compared with ATP alone (Fig. 6). Furthermore, the poststimulatory I_{sc} decrease was abolished in the presence of Na^+ channel inhibition. Na^+-free medium bathing both sides of the SMG-C6 monolayers abolished basal I_{sc} (Table III), whereas Na^+-free apical medium reversed inward basal I_{sc} to a negative value (−5.0 ± 1.1 μA/cm^2), consistent with outward cation flow (i.e., Na^+ movement from basolateral to apical bath, Table III). ATP (100 μ*M*) added to the Na^+-free apical bath induced a positive peak ΔI_{sc} (18.7 ± 2.7 μA/cm^2) with elimination of the poststimulatory I_{sc} suppression (Fig. 7). In contrast, Na^+-free basolateral medium, while maintaining apical Na^+ concentrations at ≈ 140 m*M*, did not significantly alter basal I_{sc} or R_t values; however, ATP generated a negative peak ΔI_{sc} (−7.4 ± 0.9 μA/cm^2). Therefore, the SMG-C6 epithelia exhibit stimulus-induced apical Cl^- secretion, dependent on basolateral Cl^- and Na^+; however, inward apical Na^+ transport was the predominant source of the basal current.

Expression of α-rENaC. The SMG-C6 epithelium functionally demonstrates amiloride-sensitive Na^+ transport; therefore, we determined if this cell line expresses the α-subunit from the rat epithelial Na^+ channel (α-rENaC). rENaC is composed of three subunits (α, β, and γ) and is found in rat epithelial cells such as the kidney collecting duct, the duct of several exocrine glands, and the proximal and distal airways of the lung (16). The full-length α-rENaC clone was used as a probe to hybridize in a Northern blot consisting of RNA (20 μg) from various adult rat tissues and SMG-C6 cells. A 3.8-kb transcript was identified that is consistent with α-rENaC expression in the rat submandibular glands, lung, and kidneys and in the SMG-C6 epithelia (passage 26 and 29, Fig. 8). RNA obtained from rat livers (negative control) did not express α-rENaC.

Cytokeratin Expression. Since the demonstration of amiloride-sensitive I_{sc} and expression of α-ENaC was unexpected in a submandibular cell line of acinar origin, the expression of cytokeratin 19, specific for salivary ductal epithelium (6, 11) was determined using Western analysis. Protein extracted from the SMG-C6 cells and from isolated rat submandibular glands was positively labeled with the nonspecific antipancytokeratin antibody (Fig. 9). However, cytokeratin 19 protein expression was found only in the whole submandibular gland and not identified in the SMG-C6 cells.

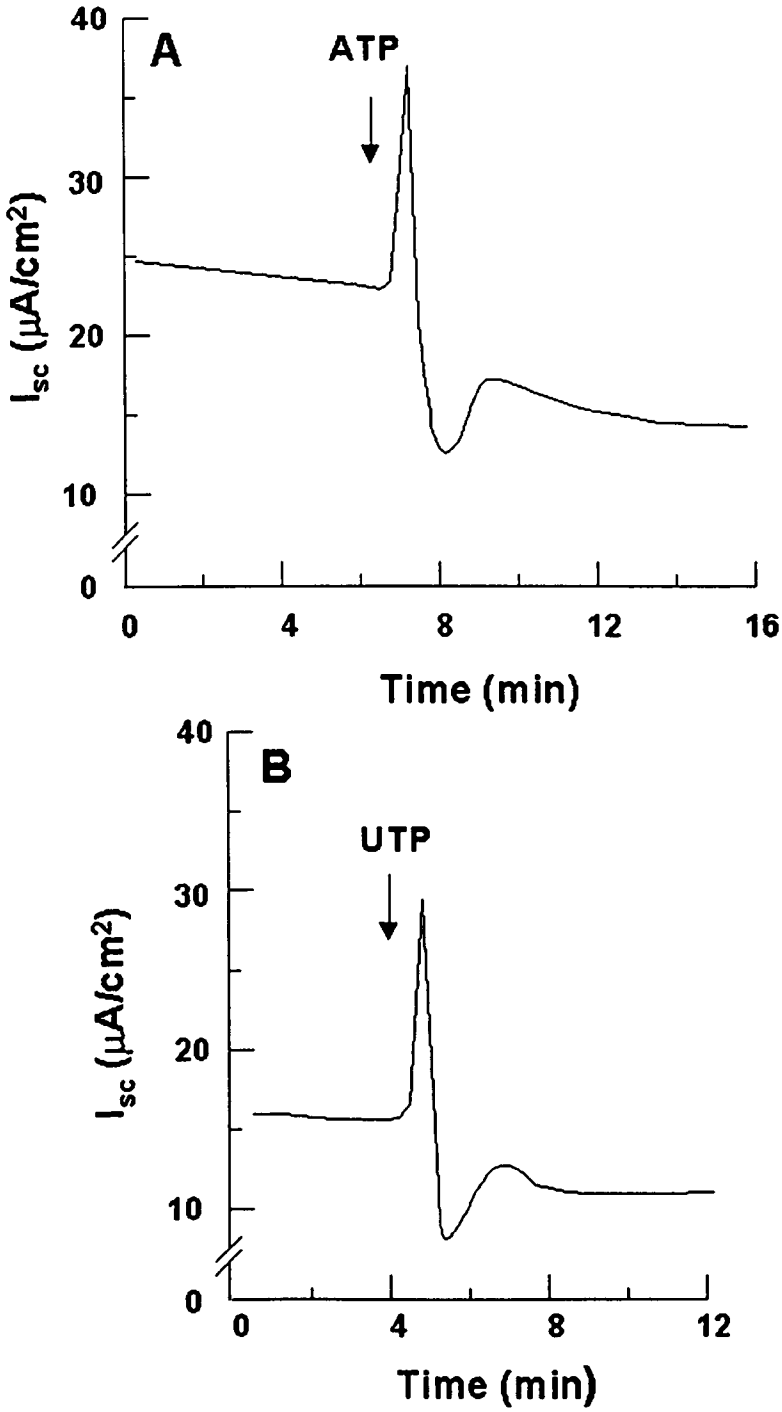

Figure 1. Representative I_{sc} tracing of the apical (A) ATP (100 μ*M*) and (B) UTP (100 μ*M*) I_{sc} (μA/cm²) response as a function of time. Filter seeded with SMG-C6 cells and mounted in Ussing chamber were treated with agents added to the apical medium (arrow).

Discussion

Salivary cells in culture serve as a useful model system to study *in vitro* the molecular and cellular biology of saliva production; however, the limited life span of primary cultured cells or the inability of tumor-derived cell lines to form polarized, tight-junction monolayers have prevented measurements of transepithelial ion movement (1, 3, 5, 17). Immortalized cell lines from rat salivary glands demonstrate structural and functional properties characteristic of *in situ* salivary epithelia, including tight junctions and localization of Na^+-K^+-ATPase proteins on the basolateral domain (6, 7). The recent characterization of neurotransmitter-regulated anion secretion in the parotid acinar cell line Par-C10 was the first report demonstrating vectorial ion transport across a salivary-derived epithelium in Ussing chambers (10).

The SMG-C6 cell line originates from the rat subman-

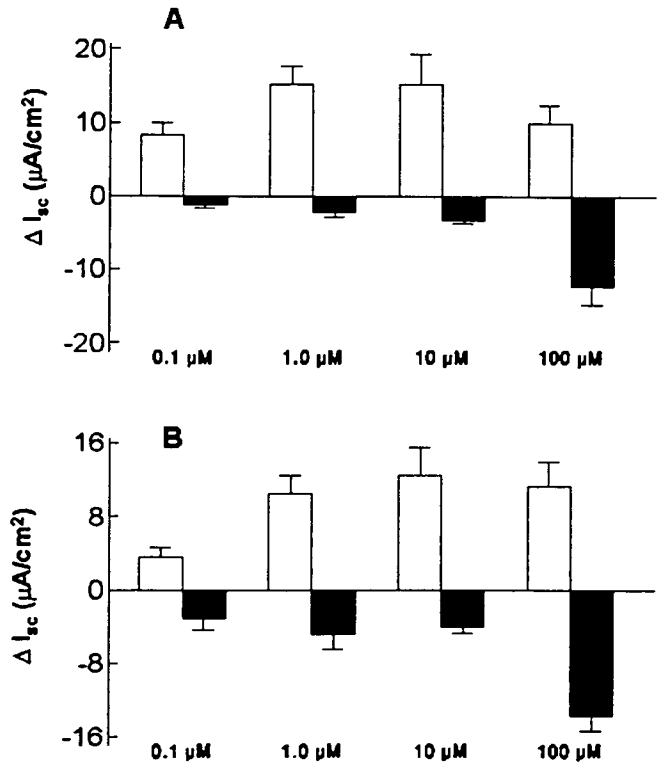

Figure 2. Immediate peak (open bar) and poststimulatory (closed bar) changes in basal I_{sc} (ΔI_{sc}, μA/cm²) in SMG-C6 epithelium in response to apical administration of (A) ATP at 0.1 μ*M* (*n* = 4), 1.0 μ*M* (*n* = 5), 10 μ*M* (*n* = 5), and 100 μ*M* (*n* = 9); and (B) UTP at 0.1 μ*M* (*n* = 4), 1.0 μ*M* (*n* = 4), 10 μ*M* (*n* = 5), and 100 μ*M* (*n* = 7). The peak and poststimulatory changes in I_{sc} values were measured within 60 sec and 20 min, respectively, following addition of P2 agonists. Values are mean ± SE.

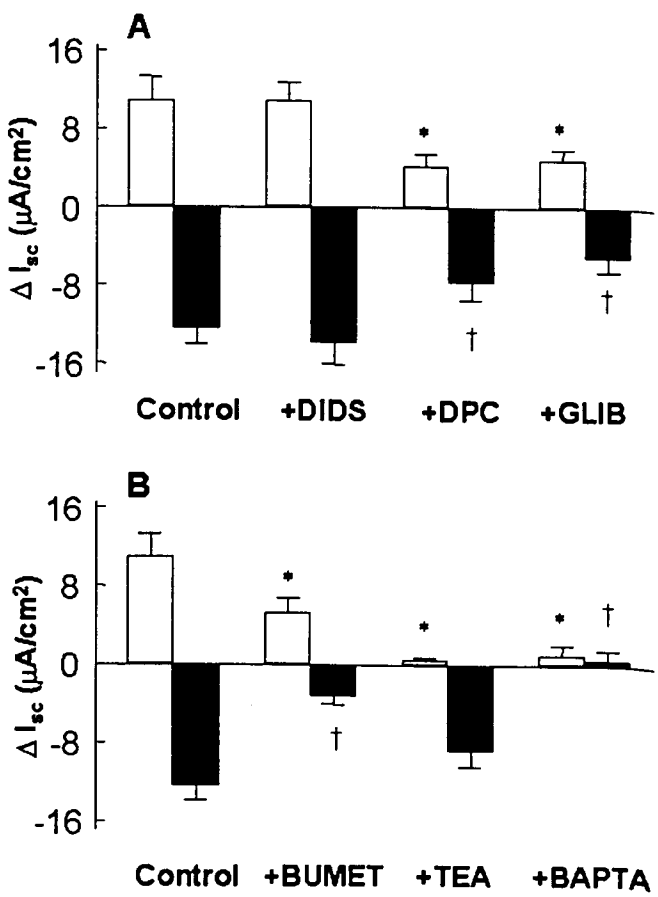

Figure 3. Immediate peak (open bar) and poststimulatory (closed bar) changes in basal I_{sc} (ΔI_{sc}, μA/cm²) across SMG-C6 epithelia in response to apical administration of ATP 100 μ*M* alone (Control, *n* = 9) and (A) following pretreatment with DIDS (100 μ*M*, *n* = 4), DPC (100 μ*M*, *n* = 6), or glibenclamide (GLIB, 100 μ*M*, *n* = 5) and (B) bumetanide (BUMET, 100 μ*M*, *n* = 4), TEA (1 m*M*, *n* = 4), or BAPTA (10 μ*M*, *n* = 5). All drugs were added to the apical media except for bumetanide and TEA. The peak and poststimulatory changes in I_{sc} values were measured within 60 sec and 20 min, respectively, following addition of P2 agonists. Values are mean ± SE; **P* < 0.05 versus control (ATP) I_{sc} peak, †*P* < 0.05 versus control (ATP) poststimulation I_{sc}.

Table III. Effects of Ion Substitution on Basal I_{sc} and R_t in SMG-C6 Monolayers

Media	*n*	I_{sc}	R_t
Krebs-bicarbonate	6	28.3 ± 2.3	615 ± 65
Cl^--free bilateral	8	41.0 ± 2.0[a]	1468 ± 157[a]
Cl^--free basolateral	4	17.0 ± 3.3[a]	1666 ± 233[a]
Na^+-free bilateral	12	0.1 ± 0.3[a]	1405 ± 263[a]
Na^+-free apical	7	-5.0 ± 1.1[a]	709 ± 72
Na^+-free basolateral	12	23.7 ± 3.3	676 ± 59

Note. Cl^- or Na^+ in Krebs-bicarbonate media was replaced with gluconate or choline, respectively. Values are mean ± SE; I_{sc}, short-circuit current (μA/cm²); R_t transepithelial resistance (Ω.cm²); *n*, number of experiments. [a] *P* < 0.05 versus Krebs-bicarbonate.

dibular acinar epithelium and shares functional properties with those found in freshly excised salivary acinar cells including activation of the IP_3-Ca^{2+} pathway by cholinergic, α-adrenergic, and P2 nucleotide receptor agonists and adenylate cyclase activation by β-adrenergic agonists (9). Employing standard culture techniques on human collagen-coated permeable supports, we found that the SMG-C6 cell line formed polarized epithelia, having transepithelial resistances of ≈ 900 Ω.cm² and a spontaneous PD of 16.9mV (apical negative). Under short-circuited conditions, ouabain added to the basolateral surface of the SMG-C6 epithelium inhibited the majority of the basal current, indicating ion transport systems dependent on Na^+-K^+-ATPase activity. Likewise, decreasing basolateral K^+ permeability with TEA may also directly inhibit Na^+-K^+-ATPase activity, resulting in a decreased basal I_{sc} (18). The lack of effect by Cl^- transport inhibition with bumetanide or removal of extracellular Cl^- suggests that basal I_{sc} was not Cl^--dependent.

The I_{sc} response to P2 nucleotide receptor agonists ATP or UTP applied to either the apical or basolateral surface was biphasic, with an initial transient peak I_{sc}, followed by a sustained I_{sc} inhibition across the SMG-C6 epithelia. The $P2Y_2$ nucleotide receptor subtype activated by UTP has been specifically localized to the apical surface of the rat salivary cell line Par-C10 (10). ATP also nonspecifically interacts with the $P2Y_2$ and other P2 receptor subtypes (10, 19). The similar I_{sc} response to UTP or ATP suggests the expression of $P2Y_2$ receptors on the SMG-C6 epithelial apical and basolateral membranes. However, it is also pos-

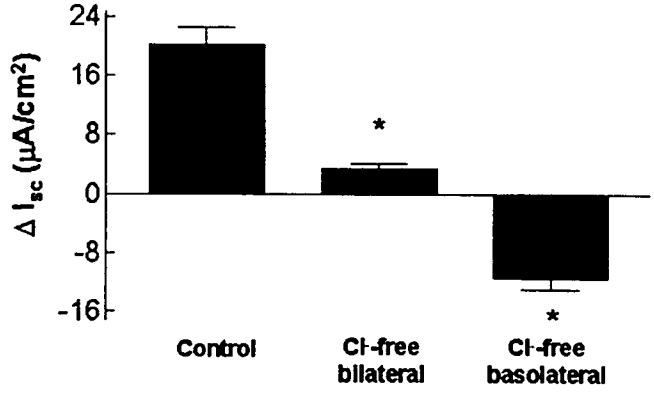

Figure 4. Change in ATP-stimulated (100 μ*M* apical) peak I_{sc} (ΔI_{sc}, μA/cm²) across SMG-C6 epithelia bathed in Krebs-Bicarbonate (KB, Control, $n = 8$), bilateral Cl^--free KB ($n = 6$), and basolateral Cl^--free KB ($n = 4$) media. Cl^- was replaced with gluconate. Apical amiloride (10 μ*M*) was present in all experimental media to inhibit basal or stimulated Na^+ transport. $^*P < 0.05$ versus control.

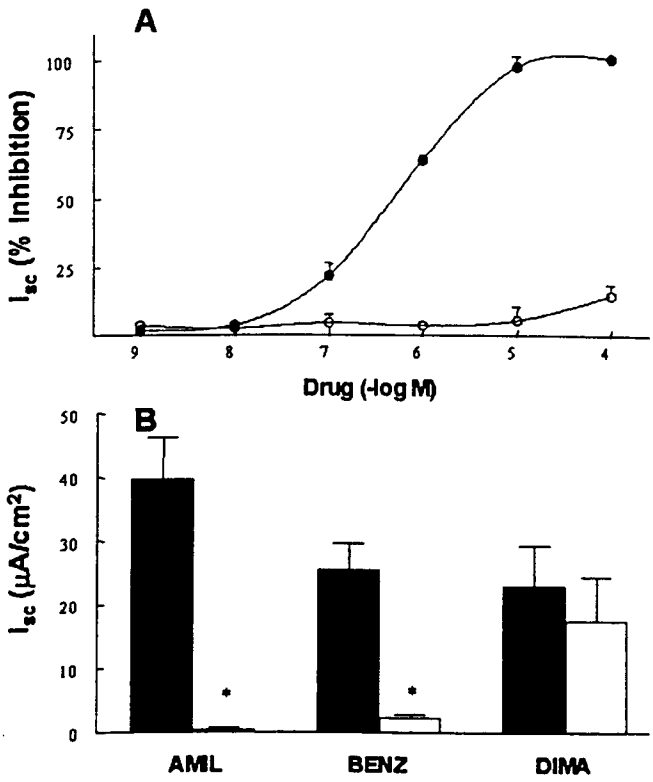

Figure 5. Effect of Na^+ transport inhibitor on basal I_{sc} across SMG-C6 epithelia. (A) Percentage (%) of basal I_{sc} inhibition across SMG-C6 epithelium in response to increasing concentrations of amiloride (closed circle, $n = 5$) and 5-(N-ethyl-N-isopropyl)-amiloride, EIPA (open circle, $n = 4$). (B) Effect of Amiloride 100 μ*M* (AMIL, $n = 8$), Benzamil 100 μ*M* (BENZ, $n = 4$) or dimethylamiloride 100 μ*M* (DIMA, $n = 4$) on basal I_{sc} (closed bar). Open bars are I_{sc} values measured after apical treatment with the above drugs. $^*P < 0.05$ versus basal I_{sc}.

sible that the agonists may have entered the contralateral medium and interacted with the receptor on the contralateral side from where they were added. In addition, without molecular biological probing for specific $P2Y_2$ messages, the possibility of other P2 receptor subtypes cannot be excluded.

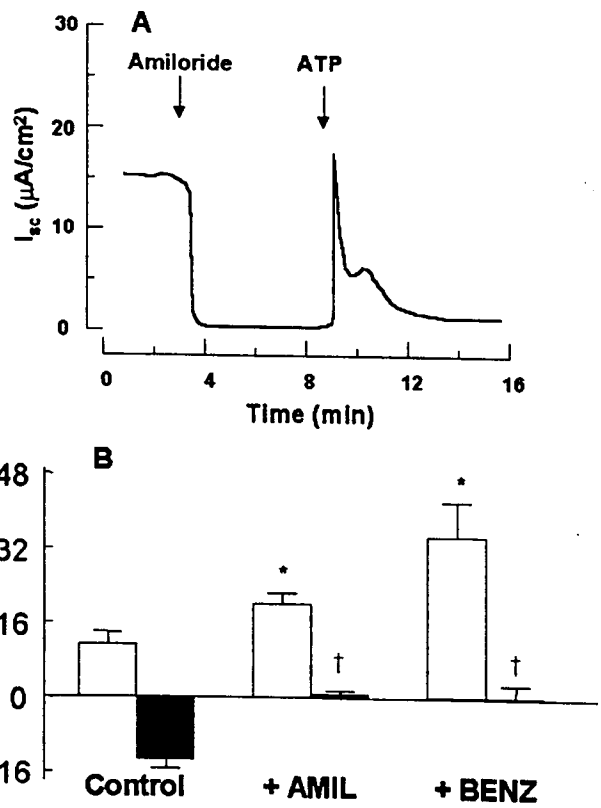

Figure 6. (A) Representative tracing of sequential addition of apical amiloride (100 μ*M*) and ATP (100 μ*M*) induced changes in SMG-C6 epithelial-generated I_{sc} as a function of time. (B) Peak (open bar) and poststimulatory (closed bar) changes in basal I_{sc} (ΔI_{sc}, μA/cm²) in response to apical administration of ATP 100 μ*M* (Control, $n = 9$) in the presence of amiloride 100 μ*M* (AMIL, $n = 8$) and benzamil 100 μ*M* (BENZ, $n = 5$). The peak and poststimulatory changes in I_{sc} values were measured within 60 sec and 20 min, respectively, following addition of P2 agonists. Values are mean ± SE; $^*P < 0.05$ versus ATP peak response, $\dagger P < 0.05$ versus ATP poststimulatory response.

The peak ΔI_{sc} responses across the SMG-C6 epithelium caused by P2 receptor agonists, representing an increase in either transepithelial cation absorption or anion secretion, were not amiloride-sensitive. However, the inhibitory effect of removing extracellular Cl^- or using specific apical Cl^- or basolateral K^+ channel blockers, suggests activation of apical Cl^- secretion (18). Cl^- uptake is maintained by the action of the basolateral Na^+-K^+-$2Cl^-$ co-transporter or through Na^+-H^+ and Cl^--HCO_3^- exchange (18). In the absence of Na^+ or Cl^- in the basolateral medium or presence of basolateral bumetanide, Cl^- entry is decreased, and the ATP-stimulated I_{sc} is diminished, further supporting activation of Cl^- secretory pathways. The ATP response was further accentuated in the presence of Na^+ channel inhibitors, amiloride and benzamil, consistent with apical membrane hyperpolarization resulting from Na^+ entry blockade, thereby increasing the electrodiffusive driving force for apical Cl^- efflux (20). Furthermore, establishing a Cl^- gradient across the SMG-C6 epithelium in the basolateral direction, ATP stimulated an inward negative peak current, consistent with apical Cl^- influx *via* ATP-activated channels (21).

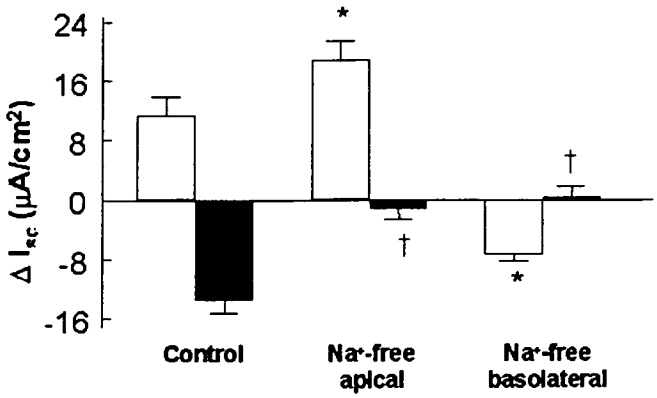

Figure 7. Effect of Na^+ replacement with choline on ATP stimulated peak and poststimulatory I_{sc} response in SMG epithelium. Filters seeded with SMG-C6 cells, placed in Ussing chambers with the following media: Krebs-Bicarbonate bilaterally (Control, $n = 9$), Na^+-free apical ($n = 12$), or Na^+-free basolateral ($n = 12$). ATP (100 μ*M*) was added apically, and the peak (open bar) and poststimulatory (closed bar) changes in I_{sc} (ΔI_{sc}, μA/cm²) are demonstrated. The peak and poststimulatory changes in I_{sc} values were measured within 60sec and 20min, respectively, following addition of P2 agonist. Values are mean ± SE. $^*P < 0.05$ versus control peak values, †$P < 0.05$ versus control poststimulatory values.

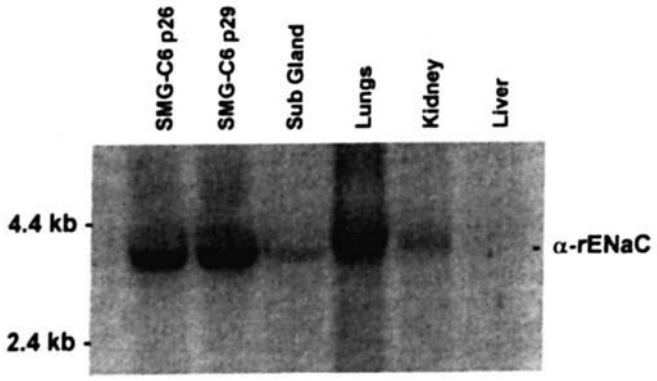

Figure 8. Northern-blot containing 20 μg/lane total RNA isolated from SMG-C6 cells (passage 26 and 29) and rat submandibular gland (sub gland), lung, kidney, and liver, hybridized with the full-length ^{32}P-labeled α-rENaC. A 3.5-kb transcript consistent with α-rENaC expression was detected in both passages from SMG-C6 cells and rat submandibular gland, lung, and kidney. No α-rENaC expression was detected in the liver.

P2 nucleotide receptor agonists stimulate intracellular Ca^{2+} mobilization in the SMG-C6 cells (9). Activation of the P2 receptors, coupled to phospholipase C, initiates increases in formation of IP_3, resulting in a rapid increase in $[Ca^{2+}]_i$ caused by release from internal stores and influx from the bathing solution (22). Since ATP induces a rapid and transient rise in both $[Ca^{2+}]_i$ and I_{sc}, activation of Ca^{2+}-dependent Cl^- channels are likely (18). Pre-incubating the SMG-C6 monolayers with BAPTA, an intracellular Ca^{2+} chelator, abolished the ATP-induced peak in I_{sc}, providing further support for activation of a Ca^{2+}-dependent Cl^- conductance by P2 nucleotide receptor agonists.

The response to ACh, a potent stimulus of Ca^{2+} mobilization and Cl^- and K^+ efflux in isolated salivary cells and intact glands (23), produced an increase in I_{sc} that was 45%

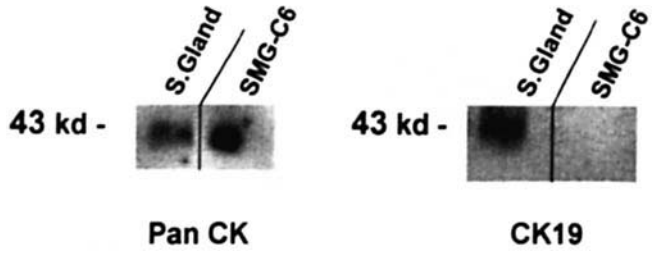

Figure 9. Western blot analysis of cytokeratin (CK) proteins from cell lysates obtained from whole rat salivary glands (S. gland) and SMG-C6 cells grown on collagen-coated culture dishes. Cell extracts were processed for Western blotting by SDS-PAGE and probed for (A) nonspecific cytokeratins (pancytokeratin-Pan CK) and (B) cytokeratin 19 (CK 19) expression. Position of molecular weight standard (in kDa) is indicated on left.

smaller than that compared with either ATP or UTP. The smaller I_{sc} response by cholinergic agonist stimulation is unclear; however, enhanced Ca^{2+} mobilization by upregulated P2 receptor subtypes has been reported in short-term culture of dispersed salivary gland cells (3). Likewise, SMG-C6 cells exposed to similar ATP or UTP concentrations caused higher elevations in $[Ca^{2+}]_i$ levels compared with cholinergic stimulation (9). It is unclear if differences in $[Ca^{2+}]_i$ elevation contribute to the differences in the I_{sc} responses to these agonists.

Stimulation with a β-adrenergic agonist generates intracellular increases in cAMP in SMG-C6 cells (9). Although β-agonists regulate secretion of amylase in salivary acinar cells and are not thought to significantly increase Cl^- conductance (18), cAMP and ATP have been shown to regulate a glibenclamide-sensitive current in salivary acinar and ductal cells (24, 25). In the present study, either isoproterenol or a cAMP-permeable analog did not alter basal I_{sc}, and no synergism between ATP and isoproterenol was evident, although the I_{sc} suppression following ATP administration alone was altered. Therefore, cAMP does not appear to alter Cl^- secretion; however, the alteration in the ATP-induced I_{sc} peak by glibenclamide found in this study suggests the presence of alternative Cl^- channel expression on the SMG-C6 apical membrane.

In the absence of Na^+ or with amiloride (10–100 μ*M*) in the apical medium, basal I_{sc} across the SMG-C6 epithelia was virtually abolished. The amiloride IC_{50} measured across the SMG-C6 epithelia is consistent with specific inhibition of Na^+ apical channels (15, 26). Higher concentrations of amiloride also inhibit the Na^+-H^+ antiport (27) in rat submandibular cells. However, benzamil's significant reduction of basal I_{sc}, in contrast with the response by amiloride analogs, dimethylamiloride or EIPA, further supports the presence of apical high-amiloride-affinity (H-type) channels (15). Amiloride or dimethylamiloride in the basolateral medium also lowered basal I_{sc}, suggesting the presence of amiloride-sensitive transport systems on the basolateral membrane. However, in the absence of Na^+ in the basolateral medium, basal I_{sc} was not altered. Therefore, the basolateral effects of these agents on basal ion transport

may reflect diffusion across the epithelium and inhibition of amiloride-sensitive Na^+ channels on the apical side.

Consistent with vectorial Na^+ transport found under I_{sc} conditions, SMG-C6 cells express α-rENaC, the major subunit of the rat epithelial Na^+ channel (28). Passive Na^+ transport into the apical or luminal direction in response to Cl^- secretion contributes to the secretory properties of the salivary acinar end pieces (18). However, amiloride-sensitive Na^+ channels, localized to kidney, lung, and colonic epithelial apical membranes (16) are not naturally expressed in submandibular acinar epithelium. Apical Na^+ channels are expressed in the salivary ducts epithelia, modifying the ion content of secondary saliva (29, 30). Despite the presence of amiloride-sensitive Na^+ conductance and expression of α-rENaC, the SMG-C6 cells do not morphologically resemble duct cells (9). Furthermore, our inability to identify cytokeratin 19 protein expression, specific for salivary ductal cells (6, 11), also does not suggest a ductal origin for this cell line. Recently, the immortalized rat parotid acinar cell line Par-C5 (8) was also found to express α-rENaC (31).

The sustained decline in I_{sc} following the transient ATP-stimulated peak I_{sc} was eliminated with the Na^+ channel blockers, amiloride or benzamil, or by removing extracellular apical Na^+. Intracellular Ca^{2+}-dependent inhibition of apical Na^+ entry has been reported in epithelia from the airways (32–36), renal collecting duct (37), and MDCK cell line (38). Likewise, an increase in cytosolic Cl^- also inhibits amiloride-sensitive Na^+ transport in salivary duct cells (29, 39). The poststimulatory ATP response in the SMG-C6 epithelia following Ca^{2+} chelation or Cl^- channel inhibition suggests a role in which changes in cytosolic Ca^{2+} or Cl^- may activate intracellular signals, altering Na^+ channel activity. Apical Na^+ channel inhibition mediated by Ca^{2+}-dependent protein kinase (40) or specific G proteins (39) has been demonstrated using patch-clamp techniques. In contrast, inhibition of Na^+ transport across human bronchial epithelium by UTP was found to be independent of PKC or PLA_2 activation (36). Increasing intracellular cAMP has also been shown to reverse partially the inhibitory effect of UTP-induced inhibition of Na^+ transport in human bronchial epithelium (36). In this study, the co-administration of ATP and isoproterenol altered the poststimulatory decrease in I_{sc} values, suggesting a similar inhibitory effect by cAMP on ATP-induced Na^+ inhibition. Intracellular cAMP regulation of Na^+ transport in this cell line is unclear; however, alteration in either ATP metabolism or desensitization of ATP-sensitive P2 receptors by cAMP occurs in tracheal submucosal epithelium (41). Finally, the entry of Na^+ ion down its electrochemical gradient is dependent on Na^+-K^+-ATPase pump activity with the recycling of K^+ across the basolateral membrane. The UTP inhibition of Na^+ transport in human bronchial epithelium was partly due to downregulation of basolateral K^+ conductance (36). In contrast, the TEA-sensitive K^+ channel on the basolateral SMG-C6 membrane did not appear to be coupled to Na^+ transport since TEA did not alter the ATP-induced sustained I_{sc} inhibition. Further studies examining the specific roles of these specific intracellular signaling elements and Na^+ transport inhibition across the SMG-C6 epithelia are needed to elucidate their underlying mechanism(s).

Salivary acini produce a Na^+ and Cl^- rich primary secretion, and the membrane components regulating fluid and electrolyte transport have been the subject of various reviews (18, 42). The SMG-C6 cell line epithelia share similar secretory properties, and the model depicted in Figure 10 summarizes the coordinated active Cl^- uptake and efflux *via* apical channels. Cholinergic (basolateral) and P2 nucleotide (apical and basolateral) receptor agonists exert their effects by stimulating the release of Ca^{2+} from intracellular stores, leading to the efflux of Cl^- through apical channels and K^+ *via* basolateral channels maintaining electroneutrality (23). This model also demonstrates the active reabsorption of Na^+ *via* amiloride-sensitive Na^+ channels that may be partly inhibited by intracellular Ca^{2+} or other downstream signaling elements. Thus, the secretory and absorptive properties exhibited by the SMG-C6 epithelia are indeed novel for *in situ* salivary epithelial ion transport processes and appear to share characteristics also found in salivary duct epithelia. Therefore, this cell line may prove to be a valuable *in vitro* model for understanding signaling mechanisms regulating fluid and electrolyte secretion and absorption in salivary and other epithelia.

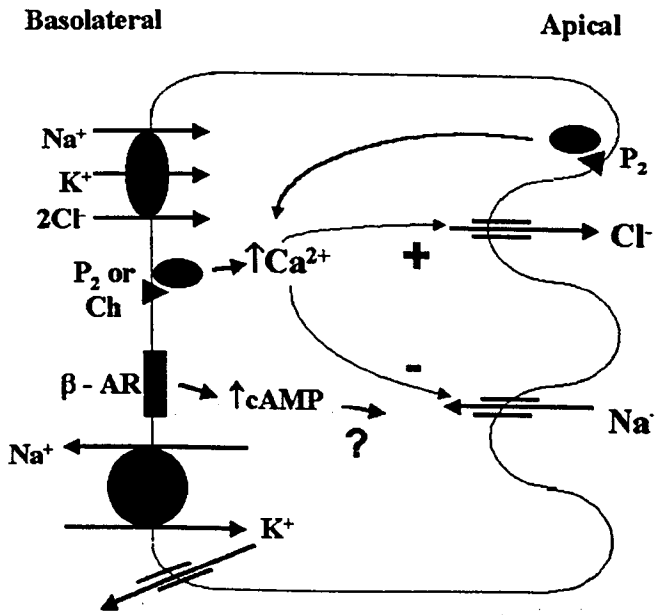

Figure 10. Schematic drawing of putative SMG-C6 epithelial transport processes involved in active Na^+ absorption and Cl^- secretion. At baseline, Na^+ enters the cells *via* specific apical channels along an inward-directed electrochemical gradient set up by basolaterally located Na^+-K^+-ATPase activity. Increased intracellular Ca^+ appears to be a negative regulator of this channel whereas the regulatory role of increases in intracellular cAMP levels resulting from β-adrenergic receptors (β-AR) activation has not been determined. Uptake of Cl^- is coupled to Na^+ *via* the Na^+-K^+-$2Cl^-$ co-transporter in the basolateral membrane. Binding of P2 nucleotide or cholinergic (Ch) agonist to specific receptors coupled to G proteins on either basolateral or apical membrane, results in an increase in intracellular Ca^{2+}, activating apical Cl^- channels and secretion into the apical medium.

We thank Dr. David O. Quissell (University of Colorado Health Science Center) for providing the SMG-C6 cell line and Dr. Hugh M. O'Brodovich and Bijan Rafii (The Hospital for Sick Children, Toronto, Ontario, Canada) for providing the α-ENaC mRNA probe and their technical assistance. We also acknowledge the excellent technical assistance of Dr. Shamin B. Mustafa and John H. Easton.

1. Quissell DO, Redman RS, Mark MR. Short-term primary culture of acinar-intercalated duct complexes from rat submandibular glands. *In Vitro* Cell Dev Biol **22**:469–480, 1986.
2. Sabatini LM, Allen-Hoffmann BL, Warner TF, Azen EA. Serial cultivation of epithelial cells from human and macaque salivary glands. *In Vitro* Cell Dev Biol **27A**:939–948, 1991.
3. Turner JT, Weisman GA, Camden JM. Upregulation of $P2Y_2$ nucleotide receptors in rat salivary gland cells during short-term culture. Am J Physiol **273**:C1100–C1107, 1997.
4. Yeh C-K, Mertz PM, Olivers C, Baum BJ, Kousvelari EE. Cellular characteristics of long-term cultured rat parotid acinar cells. *In Vitro* Cell Dev Biol **27A**:707–712, 1991.
5. Zhu Y, Aletta JM, Wen J, Zhang X, Higgins D, Rubin RP. Rat serum induces a differentiated phenotype in a rat parotid acinar cell line. Am J Physiol **275**:G259–G268, 1998.
6. Laoide BM, Courty Y, Gastinne I, Thibaut C, Kellermann O, Rougeon F. Immortalized mouse submandibular epithelial cell lines retain polarized structural and functional properties. J Cell Sci **109**:2789–2800, 1996.
7. He X, Kuijpers GAJ, Goping G, Kulakusky JA, Zheng C, Delporte C, Tse CM, Redman RS, Donowitz M, Pollard HB, Baum BJ. A polarized salivary cell monolayer useful for studying transepithelial fluid movement *in vitro*. Pflugers Arch **435**:375–381, 1998.
8. Quissell DO, Barzen KA, Redman RS, Camden JM, Turner JT. Development and characterization of SV40 immortalized rat parotid acinar cell lines. *In Vitro* Cell Dev Biol **34**:58–67, 1998.
9. Quissell DO, Barzen KA, Gruenert DC, Redman RS, Camden JM, Turner JT. Development and characterization of SV40 immortalized rat submandibular acinar cell lines. *In Vitro* Cell Dev Biol **33**:164–173, 1997.
10. Turner JT, Redman RS, Camden JM, Landon LA, Quissell DO. A rat parotid gland cell line, Par-C10, exhibits neurotransmitter-regulated transepithelial anion secretion. Am J Physiol **275**:C367–C374, 1998.
11. Geiger S, Geiger B, Leitner O, Marshak G. Cytokeratin polypeptides expression in different epithelial elements of human salivary glands. Virchows Arch A Pathol Anat Histopathol **410**:403–414, 1987.
12. O'Brodovich H, Canessa C, Ueda J, Rafii B, Rossier BC, Edelson J. Expression of the epithelial Na^+ channel in the developing rat lung. Am J Physiol **265**:C491–C496, 1993.
13. Dinudom A, Komwatana P, Young JA, Cook DI. A forskolin-activated Cl^- current in mouse mandibular duct cells. Am J Physiol **268**:G806–G812, 1995.
14. Ishikawa T, Cook DI. A Ca^{2+}-activated Cl^- current in sheep parotid secretory cells. J Membr Biol **135**:261–271, 1993.
15. Kleyman TR, Cragoe EJ. Amiloride and its analogs, as tools in the study of ion transport. J Membr Biol **105**:1–21, 1988.
16. Benos DJ, Awayda MS, Ismailov II, Johnson JP. Structure and function of amiloride-sensitive Na^+ channels. J Membr Biol **143**:1–18, 1995.
17. Horie K, Kagami H, Hiramatsu Y, Hata K, Shigetomi T, Ueda M. Selected salivary-gland cell culture and the effects of isoproterenol, vasoactive intestinal polypeptide, and substance P. Arch Oral Biol **41**:243–252, 1996.
18. Cook DI, Van Lennep EW, Roberts ML, Young JA. Secretion by the major salivary glands. In: Johnson LR, Ed. Physiology of the Gastrointestinal Tract. New York: Raven Press, pp1061–1117, 1994.
19. Turner JT, Landon LA, Gibbons SJ, Talamo BR. Salivary gland P2 nucleotide receptors. Crit Rev Oral Biol Med **10**:210–224, 1999.
20. Cotton CU, Boucher RC, Gatzy JT. Paths of ion transport across canine fetal tracheal epithelium. J Appl Physiol **65**:2376–2382, 1988.
21. Sheppard DN, Carson MR, Ostedgaard LS, Denning GM, Welsh MJ. Expression of cystic fibrosis transmembrane conductance regulator in a model epithelium. Am J Physiol **266**:L405–L413, 1994.
22. Boarder MR, Weisman GA, Turner JT, Wilkinson GF. G-protein coupled P2 purinoceptors: From molecular biology to functional responses. Trends Pharmacol Sci **16**:133–139, 1995.
23. Martinez JR, Camden J, Kingsbury MB. Effects of acetylcholine and transport inhibitors on K^+ content in dispersed submandibular salivary cells of newborn and adult rats. Arch Oral Biol **33**:203–207, 1988.
24. Zeng W, Lee MG, Yan M, Diaz J, Marino CR, Muallem S. Immuno and functional characterization of CFTR in submandibular and pancreatic acinar and duct cells. Am J Physiol **273**:C442–C455, 1997.
25. Zeng W, Lee MG, Muallem S. Membrane-specific regulation of Cl^- channels by purinergic receptors in rat submandibular gland acinar and duct cells. J Biol Chem **272**:32956–32965, 1997.
26. Cheek JM, Kim K-J, Crandall ED. Tight monolayers of rat alveolar epithelial cells: Bioelectric properties and active sodium transport. Am J Physiol **256**:C688–C693, 1989.
27. Lee MG, Schultheis PJ, Yan M, Shull GE, Bookstein C, Chang E, Tse M, Donowitz M, Park K, Muallem S. Membrane-limited expression and regulation of Na^+-H^+ exchanger isoforms by P2 receptors in the rat submandibular gland duct. J Physiol **513**:341–357, 1998.
28. Champigny G, Voilley N, Lingueglia E, Friend V, Barbry P, Lazdunski M. Regulation of expression of the lung amiloride-sensitive Na^+ channel by steroid hormones. EMBO J **13**:2177–2181, 1994.
29. Bijman J, Cook DI, van Os CH. Effect of amiloride on electrolyte transport parameters of the main duct of the rabbit mandibular salivary gland. Pflugers Arch **398**:96–102, 1983.
30. Dinudom A, Young JA, Cook DI. Amiloride-sensitive Na^+ current in the granular duct cells of mouse mandibular glands. Pflugers Arch **423**:164–166, 1993.
31. Zentner MD, Lin HH, Wen X, Kim KJ, Ann DK. The amiloride-sensitive epithelial sodium channel α-subunit is transcriptionally downregulated in rat parotid cells by the extracellular signal-regulated protein kinase pathway. J Biol Chem **273**:30770–30776, 1998.
32. Al-Bazzaz FJ. Regulation of Na and Cl transport in sheep distal airways. Am J Physiol **267**:L193–L198, 1994.
33. Iwase N, Sasaki T, Shimura S, Yanamoto M, Suzuki S, Shirato K. ATP-induced Cl^- secretion with suppressed Na^+ absorption in rabbit tracheal epithelium. Respir Physiol **107**:173–180, 1997.
34. Acevedo M. Effect of acetyl choline on ion transport in sheep tracheal epithelium. Pflugers Arch **427**:543–546, 1994.
35. Van Scott MR, Paradiso AM. Intracellular Ca^{2+} and regulation of ion transport across rabbit Clara cells. Am J Physiol **263**:L122–L127, 1992.
36. Devor DC, Pilewski JM. UTP inhibits Na^+ absorption in wild-type and ΔF508 CFTR-expressing human bronchial epithelia. Am J Physiol **276**:C827–C837, 1999.
37. Koster HP, Hartog A, van Os CH, Bindels RJ. Inhibition of Na^+ and Ca^{2+} reabsorption by P2u purinoceptors requires PKC but not Ca^{2+} signaling. Am J Physiol **270**:F53–F60, 1996.
38. Ishikawa T, Marunaka Y, Rotin D. Electrophysiological characterization of the rat epithelial Na^+ channel (rENaC) expressed in MDCK cells. Effects of Na^+ and Ca^{2+}. J Gen Physiol **111**:825–846, 1998.
39. Dinudom A, Komwatana P, Young JA, Cook DI. Control of the amiloride-sensitive Na^+ current in mouse salivary ducts by intracellular anions is mediated by a G protein. J Physiol **487**:549–555, 1995.
40. Frindt G, Palmer LG, Windhager EE. Feedback regulation of Na channels in rat CCT. IV. Mediation by activation of protein kinase C. Am J Physiol **270**:F371–F376, 1996.
41. Shimura S, Sasaki T, Nagaki M, Takishima T, Shirato K. Extracellular ATP regulation of feline tracheal submucosal gland secretion. Am J Physiol **267**:L159–L164, 1994.
42. Martinez JR. Cellular mechanisms underlying the production of primary secretory fluid in salivary glands. Crit Rev Oral Biol Med **1**:67–78, 1990.